**OPEN ACCESS**

Original research

# Anterior limb of the internal capsule tractography: relationship with capsulotomy outcomes in obsessive-compulsive disorder

Chencheng Zhang [ID],[1] Seung-Goo Kim,[2,3] Jun Li [ID],[1] Yingying Zhang,[1] Qiming Lv,[4,5] Kristina Zeljic,[4,5] Hengfen Gong,[6] Hongjiang Wei,[7] Wenjuan Liu,[8] Bomin Sun,[1] Zheng Wang,[5,9] Valerie Voon[2]

## ABSTRACT

**Objectives** Surgical procedures targeting the anterior limb of the internal capsule (aLIC) can be effective in patients with selected treatment-refractory obsessive-compulsive disorder (OCD). The aLIC consists of white-matter tracts connecting cortical and subcortical structures and show a topographical organisation. Here we assess how aLIC streamlines are affected in OCD compared with healthy controls (HCs) and which streamlines are related with post-capsulotomy improvement.

**Methods** Diffusion-weighted MRI was used to compare white-matter microstructure via the aLIC between patients with OCD (n=100, 40 women, mean of age 31.8 years) and HCs (n=88, 39 women, mean of age 29.6 years). For each individual, the fractional anisotropy (FA) and streamline counts were calculated for each white-matter fibre bundle connecting a functionally defined prefrontal and subcortical region. Correlations between tractography measures and pre-capsulotomy and post-capsulotomy clinical outcomes (in obsessive-compulsive, anxiety and depression scores 6 months after surgery) were assessed in 41 patients with OCD.

**Results** Hierarchical clustering dendrograms show an aLIC organisation clustering lateral and dissociating ventral and dorsal prefrontal–thalamic streamlines, findings highly relevant to surgical targeting. Compared with HCs, patients with OCD had lower aLIC FA across multiple prefrontal cortical–subcortical regions (p<0.0073, false discovery rate-adjusted). Greater streamline counts of the dorsolateral prefrontal–thalamic tracts in patients with OCD predicted greater post-capsulotomy obsessive-compulsive improvement (p=0.016). In contrast, greater counts of the dorsal cingulate–thalamic streamlines predicted surgical outcomes mediated by depressive and anxiety improvements.

**Conclusions** These findings shed light on the critical role of the aLIC in OCD and may potentially contribute towards precision targeting to optimise outcomes in OCD.

## INTRODUCTION

The pathophysiology of obsessive-compulsive disorder (OCD) implicates cortico–striato–thalamic networks[1 2] whose tracts course through the anterior limb of the internal capsule (aLIC), a key white-matter structure in this network.[3 4] Diffusion tensor imaging (DTI) studies in OCD have shown heterogeneous findings but suggest white-matter abnormalities in patients with OCD in the cingulate bundle, the corpus callosum and the aLIC.[5–9]

Capsulotomy and deep brain stimulation targeting the aLIC and subthalamic nucleus (STN) can be effective in alleviating the clinical symptoms of severe medical-refractory patients with OCD.[10–13] Capsulotomy is a neurosurgical procedure involving ablation with radiothermy, gamma knife or high-frequency ultrasound of the aLIC, and reduces OCD symptoms by an average of a little over 50% with a range of 37%–80%.[14 15] A single-shot ablative lesion targeting the mid-aLIC is less effective than a further lesion expansion using 'double-shot' or 'triple-shot' techniques which include the ventral aLIC.[12 16] Thus, clinical outcome studies tracking the effects of ventral–dorsal location are crucial for assessing which tracts through the aLIC connecting cortical and subcortical structures may be most clinically relevant in predicting capsulotomy outcomes.

Converging evidence from primate tract tracing and human DTI studies shows that different regions of the aLIC carry fibres from different prefrontal regions with a ventral–dorsal, medial–lateral and anterior–posterior organisational topography.[3 4] Imaging studies have highlighted specific tracts and connections for predicting postoperative clinical outcomes. A preoperative tractography study following ventral internal capsule deep brain stimulation (VIC DBS) showed that the most clinically effective contacts stimulated thalamo–cortical aLIC fibres to the dorsolateral prefrontal cortex (dlPFC), rostral dorsal anterior cingulate (dACC) and mesial PFC.[17] In a second study comparing preoperative tractography in VIC and STN DBS for OCD, similar aLIC fibre streamlines were identified to the rostral cingulate and mesial PFC across both DBS targets as predictive of optimal clinical outcome.[18] Furthermore, a predictive resting state functional MRI (fMRI) study of capsulotomy outcomes from our group highlighted functional connectivity between the dorsal cingulate and striatum as predictive of obsessive-compulsive symptom improvement 1 month after surgery.[19] These studies investigating the predictive role of imaging are potentially critical in guiding more precise neurosurgical targeting,[20]

BMJ

and suggest particular abnormality of white-matter tracts passing through the aLIC may exist in OCD and may also be related with clinical outcome by neurosurgery targeting at aLIC.

The goal of the present study was twofold: first, we identified which cortical–subcortical white-matter streamlines passing through the aLIC were abnormal in OCD. Here, we focused on specific functionally defined prefrontal regions implicated in OCD including dlPFC, orbitofrontal cortex (OFC), ventrolateral PFC (vlPFC) (or inferior frontal cortex), dACC and ventromedial (vmPFC), which were used in our previous studies.[21 22] These cortical regions have been suggested to be impaired in OCD based on convergent cognitive, task-based fMRI studies related to decision-making and impulsivity.[1 2] Here, using a tractographic analysis, we focused on the quantitative characteristics of the white matter streamlines via the aLIC of these prefrontal regions connecting to subcortical regions of striatum, thalamus and STN in OCD. Second, focusing on the regions shown to be predictive of capsulotomy and DBS outcomes, namely the dlPFC and dACC,[17–19] we ask in a subset of these patients whether these streamlines are correlated with improvements in obsessive-compulsive, depressive and anxiety symptoms following capsulotomy for severe treatment-refractory OCD.

## MATERIALS AND METHODS
### Subjects and clinical assessment
Patients with OCD who were considered for neurosurgery at Ruijin Hospital from August 2013 to September 2018 were recruited in the imaging study (n=100). Age and gender-matched healthy controls (HCs) were recruited via community-based advertisements (n=88). OCD diagnosis was confirmed using the Diagnostic and Statistical Manual of Mental Disorders-IV-TR criteria by a psychiatrist specialising in OCD. Exclusion criteria for patients and for age-matched and gender-matched HCs for imaging included: age below 16 or above 65, a history of severe head trauma, substance use disorders, other major psychiatric or major neurological disorders, claustrophobia, and metal or electronic implants. Inclusion criteria and surgical details for capsulotomy have been previously reported.[19] Inclusion for capsulotomy included a Yale-Brown Obsessive Compulsive Scale (Y-BOCS) score of more than 25 or one subscale of more than 15; chronicity of greater than 5 years; treatment refractory defined as more than three antidepressant trials of greater than 12 weeks at maximally tolerated doses and adequate failed psychotherapy. Clinical information was collected using the Y-BOCS, Hamilton Anxiety Rating Scale (HAM-A) and the 17-item version of Hamilton Depression Rating Scale (HAM-D).

### Capsulotomy and follow-up
Among the patients with OCD (n=100) included in the current study, 78 underwent capsulotomy.

Details of the surgical procedure can be found in our previous work[19] and are briefly summarised here. A stereotactic frame was mounted on the patient's head under local anaesthesia, and preoperative MRI was immediately scanned. The target was localised between the anterior and middle thirds of the aLIC. Stereotactic target coordinates and the trajectory angle for the target region were calculated according to stereotactic MRI. The radiofrequency lesions were generated by radiofrequency ablation with a 2 mm diameter electrode at 75℃ for 60 s, and a lesion region 4–5 mm in diameter and 10–12 mm in length along the contoured target was produced.

After surgery (n=78), 41 completed assessments at least 6 months after surgery (data included in the analyses related to postsurgical improvement), 11 completed assessments between 1 and 5 months after surgery and 26 either could not be contacted after surgery or were unable to attend a follow-up visit.

### Image acquisition
Diffusion-weighted imaging was conducted on a Siemens Tim Trio 3-Tesla scanner (Siemens, Erlangen, Germany) using a 12-channel phased-array head coil. A diffusion spectrum imaging (DSI) sequence was acquired with a total of 515 diffusion directions covering a hemisphere with the maximum b-value of $7000 \, s/mm^2$ (field of view=$192 \times 192 \, mm^2$, matrix size=$80 \times 80$, in-plane resolution=2.4 mm, slice thickness=2.4 mm, repetition time=10 100 ms, echo time=152 ms, flip angle=90°, in-plane acceleration factor=2).[23] Due to low signal-to-noise ratio (SNR) at high b-values, only 171 directions up to the b-value of $4800 \, s/mm^2$ were used in further analyses. A T1-weighted image was also collected with a magnetisation prepared rapid gradient-echo sequence (field of view=$256 \times 256 \, mm^2$, matrix size=$256 \times 256$, in-plane resolution=1 mm, slice thickness=1 mm, repetition time=2300 ms, echo time=3 ms, inversion time=1000 ms, flip angle=9°).

### Denoising, diffusion modelling and deterministic tractography
As the diffusion data were DSI rather than DTI with low SNR with very high b-values and in the ventromedial prefrontal regions, we adapted our processing and analytic algorithm specifically for these issues. We used local principal component analysis (local PCA) for denoising of the diffusion-weighted images (https://sites.google.com/site/pierrickcoupe/softwares/denoising-for-medical-imaging/dwi-denoising/dwi-denoising-software).[24] PCA was performed on a sliding local-block at each voxel over diffusion directions and the data were reconstructed without noisy components as determined by their associated eigenvalues (see online supplemental figure 1 for denoising). Eddy current correction could not be applied as it is not implemented for DSI data in any publicly available software (eg, see https://fsl.fmrib.ox.ac.uk/fsl/fslwiki/eddy/UsersGuide#A--data_is_shelled).

The denoised diffusion data were analysed using DSI Studio (http://dsi-studio.labsolver.org). The SNR, particularly in the frontal areas, was low, thus a high-order model such as generalised q-sampling imaging[25] resulted in implausible and spurious results. A lower-order model is less sensitive to such noise because it does not model complex functions and only more general trends. Therefore, we sacrificed the high angular resolution to improve SNR by fitting with a traditional Gaussian tensor with only three orthogonal axes. Based on the tensor models, we used a deterministic fibre tracking algorithm[26] to find tract bundles connecting pairs of cortical and subcortical regions of interest (ROIs) seeding from all voxels within the aLIC. The deterministic approach was chosen to find the best estimation with computational efficiency over the probabilistic approach.[27] The aLIC was defined using the Harvard-Oxford atlas in FSL (FSL-HO (https://fsl.fmrib.ox.ac.uk/fsl/fslwiki/Atlases)).[28] Six cortical ROIs (figure 1) were included: vlPFC, dlPFC, vmPFC, dACC, pre-supplementary motor area (pre-SMA) and OFC. The ROIs of the vlPFC, dlPFC, vmPFC, dACC and pre-SMA were manually defined and used in previous publications from our group (see online supplemental materials in Morris et al for more details on manual definitions).[21 22] Five subcortical ROIs (figure 1) were included: thalamus, caudate, putamen, nucleus accumbens (NAcc) and STN. The ROIs of the OFC, thalamus, caudate nuclei, putamen and NAcc were identified using the
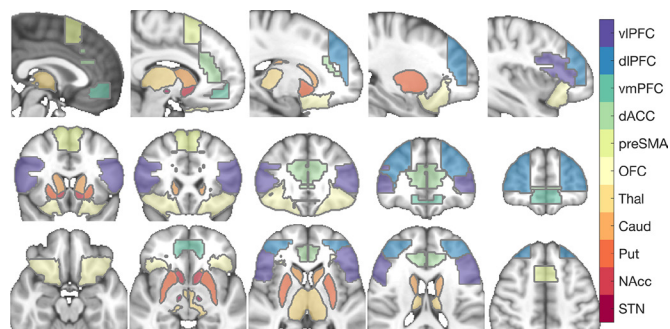
**Figure 1** Regions of interest. Caud, caudate nucleus; dACC, dorsal anterior cingulate cortex; dlPFC, dorsolateral prefrontal cortex; OFC, orbitofrontal cortex; NAcc, nucleus accumbens; pre-SMA, anterior portion of supplementary motor area; Put, putamen; STN, subthalamic nucleus; Thal, thalamus; vlPFC, ventrolateral prefrontal cortex; vmPFC, ventromedial prefrontal cortex.

FSL-HO atlas. The ROI of the STN was defined using the multi-contrast PD25 atlas (http://nist.mni.mcgill.ca/?p=1209).[29] All ROIs and the seed masks were defined in Montreal Neurological Institute template space and non-linearly transformed into individual diffusion spaces using the unified segmentation in SPM12 (see online supplemental figure 2 for examples of the registrations of ROIs).

For each cortical and subcortical ROI pair, a seeding region was placed at the aLIC in both hemispheres, and 1 000 000 streamlines were generated. The angular threshold was set to 60° and the step size to 0.5 mm. The fractional anisotropy (FA) threshold was 0.05 in accordance with the relatively low SNR of the current data. The fibre trajectories were then smoothed by averaging the propagation direction with 50% of the previous direction. Tracks <30 mm or >300 mm were discarded.

### Statistical inference
From the tractography results, normalised streamline counts (NC) of streamlines ending in the ROIs (normalised by their lengths) and averaged FA of the streamlines were calculated. In some connections, a proportion of subjects showed no streamlines. To enhance the reliability of the analysis, we focused only on the 12 connections in which more than 90% of subjects showed streamlines. For each connection, only subjects with connections were included in the analysis resulting in varying df across connections.

We tested our main objectives using the following general linear models (GLMs) asking: (i) whether OCD and HC groups differ in measures of white matter fibre connectivity; (ii) whether improvements in clinical measures (Y-BOCS, HAM-A, HAM-D) >6-month follow-up post-capsulotomy (ie, postminus-presurgery) correlate with measures of white matter fibre connectivity of the thalamus with dlPFC and dACC.[17–19]

$$y = \beta_0 + \beta_1 \text{Age} + \beta_2 \text{Gender} + \beta_3 \text{TIV} + \beta_4 \text{OCD} + \text{error} \quad (1)$$
$$y = \beta_0 + \beta_1 \text{Age} + \beta_2 \text{Gender} + \beta_3 \text{TIV} + \beta_4 \left( x_{\text{follow-up}} - x_{\text{baseline}} \right) + \text{error} \quad (2)$$

where y is a connectivity measure (either NC or FA), TIV is total intracranial volume, OCD is a binary variable indicating patients with OCD or HC status, x is a clinical measure (either Y-BOCS, HAM-A, or HAM-D) at either baseline or follow-up, error is unknown noise, and betas are unknown coefficients estimated by the ordinary least square method. The TIV was estimated from T1-weighted images using the Segment module and the Tissue Volume utility in SPM12 (http://www.fil.ion.ucl.ac.uk/spm).[30] In order to assess the effect of group membership or clinical measures while regressing out the effects of covariates, a t-statistic is calculated from $t = \frac{c^T \hat{\beta}}{\sqrt{\hat{\sigma}^2 c^T (X^T X)^{-1} c}}$ where c is a contrast vector $[0, 0, 0, 0, 1]^T$, $\sigma^2$ is a sample variance and X is a design matrix.

Multicollinearity of regressors was assessed using a MATLAB implementation (https://github.com/brian-lau/colldiag). For model (1), CIs did not exceed 11 with only weak collinearity between Y-BOCS baseline scores and TIV (CI=11, variance decomposition proportions (VDPs)=82.5%, 90.1%). For model (2), CIs did not exceed 12 (age and TIV, CI=12, VDPs=96.2%, 96.2%). Overall, there was only weak collinearity between age and TIV well below a threshold of 30.[31]

P values were estimated using the Monte Carlo method (100 000 permutations) as implemented in the FieldTrip MATLAB Toolbox (http://www.fieldtriptoolbox.org/), with a false discovery rate (FDR) adjustment for multiple comparisons when necessary. A family-wise alpha level of 0.05 was used.

### Tract-based spatial statistics
In order to assess whether our group findings of streamlines within the aLIC were specific to the aLIC or more generalised white matter differences between OCD and HC groups, we also conducted an analysis of local diffusion properties in a voxel-wise fashion using whole-brain tract-based spatial statistics (TBSS) in FSL.[32] FA images were non-linearly registered to the FMRIB58_FA template, skeletonised and thresholded at 0.05. We focused here on FA as our aLIC measures focus on FA. Note that the range of the FA estimates was lower than usual DTI data. Two GLMs (equations 1–2) were non-parametrically tested using threshold-free cluster enhancement,[33] as implemented in *randomise* in FSL, with 10 000 permutations each. Family-wise alpha level of 0.05 was used.

Unless otherwise noted, custom MATLAB (R2019a V.9.6.0.1135713; MathWorks, Natick, Massachusetts, USA) functions were used. Streamline visualisation was conducted using DSI-Studio.

## RESULTS
### Demographic and clinical measures
The patients with OCD (n=100; 31.8 (SD 9.7) years old) and HCs (n=88; 29.6 (SD 8.0) years old) were matched in age (t=−1.64, p=0.102), gender (OCD female ratio 0.40; HC 0.44; $\chi^2$=0.21; p=0.649) and total intracranial volume (OCD in litres 1.45 (SD 0.13); HC 1.42 (SD 0.14); t=−1.55; p=0.122). Clinical measures and obsessive-compulsive symptoms at different time points are reported in table 1 and online supplemental table 1. The 41 patients who underwent capsulotomy and completed assessments at least 6 months after surgery were included in the analyses related to postsurgical improvement. The YBOCS, HAMD and HAMA scores decreased post-capsulotomy (one-sample t-test, p<0.0001) (online supplemental figure 3).

## TRACTOGRAPHY
### General tractography and group comparison
The number of subjects that showed any streamlines varied across connections between cortical and subcortical ROIs (online supplemental table 2). Streamlines were found in more than 90% of subjects (>169) for 12 connections: (i) thalamus–vlPFC, (ii) thalamus–dlPFC, (iii) thalamus–dACC, (iv) thalamus–pre-SMA,

**Table 1** Clinical measures of patients with OCD

| | n | Mean | SD | Min | Max |
|---|---|---|---|---|---|
| Duration of illness (year) | 84 | 10.3 | 5.8 | 1 | 25 |
| Age at onset of illness (year) | 79 | 21.0 | 8.6 | 7 | 53 |
| Y-BOCS (baseline: all patients with OCD) | 96 | 30.4 | 6.7 | 15 | 40 |
| Y-BOCS (baseline: ≥6-month follow-up patients) | 41 | 30.1 | 7.1 | 15 | 40 |
| Y-BOCS (follow-up: ≥6-month follow-up patients) | 41 | 12.7 | 12.0 | 0 | 38 |
| Y-BOCS follow-up time after surgery (month) | 41 | 25.8 | 23.0 | 6 | 91 |
| HAM-A (baseline: all patients with OCD) | 94 | 17.8 | 10.0 | 0 | 46 |
| HAM-A (baseline: ≥6-month follow-up patients) | 41 | 17.3 | 9.2 | 2 | 40 |
| HAM-A (follow-up: ≥6-month follow-up patients) | 41 | 10.6 | 8.5 | 0 | 31 |
| HAM-A follow-up time after surgery (month) | 41 | 25.8 | 23.0 | 6 | 91 |
| HAM-D (baseline: all patients with OCD) | 91 | 14.5 | 7.2 | 0 | 31 |
| HAM-D (baseline: ≥6-month follow-up patients) | 38 | 14.3 | 6.7 | 3 | 29 |
| HAM-D (follow-up: ≥6-month follow-up patients) | 38 | 8.4 | 6.3 | 0 | 22 |
| HAM-D follow-up time after surgery (months) | 38 | 23.3 | 19.4 | 6 | 69 |

The 41 patients who underwent capsulotomy and were clinically assessed at least 6 months after surgery were included in the follow-up.

HAM-A, Hamilton Anxiety Rating Scale; HAM-D, Hamilton Depression Rating Scale; n, number of available data points out of 100 patients with OCD; Y-BOCS, Yale–Brown Obsessive Compulsive Scale.

(v) thalamus–OFC, (vi) caudate–dlPFC, (vii) putamen–vlPFC, (viii) putamen–dlPFC, (ix) putamen–pre-SMA, (x) STN–vlPFC, (xi) STN–dlPFC, (xii) STN–pre-SMA. See figure 2 for averaged track density images and an illustration of the streamlines between cortical and subcortical regions. For each connection (including those found in <90% of subjects), the proportion of subjects who showed streamlines was similar between OCD and HC groups ($\chi^2$ tests; p>0.4395, uncorrected; p>0.9773, FDR-adjusted). We also assessed the relationship between streamline measures (FA or NC) and baseline clinical severity (ie, baseline YBOCS/HAM-D/HAM-A scores) or obsessive-compulsive symptom subtypes (online supplemental table 1); there were no significant findings and hence are not reported here.

We then asked whether the identified aLIC streamlines were spatially segregated within the aLIC, an important question relevant to surgical targeting. Across all subjects, spatial distributions
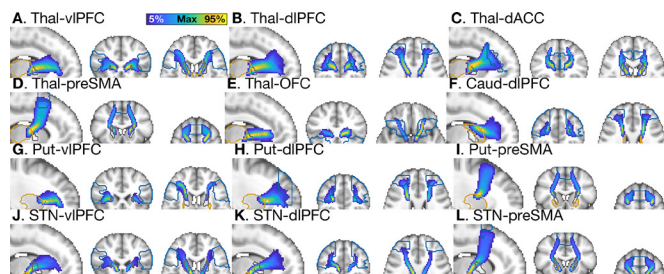


**Figure 2** Maximal intensity projection of averaged track-density images. Colour coding is scaled proportionally to the maximal density. Cortical (orange) and subcortical (blue) ROIs and aILCs (grey) are marked in contours. Regions of interest. Caud, caudate nucleus; dACC, dorsal anterior cingulate cortex; dlPFC, dorsolateral prefrontal cortex; OFC, orbitofrontal cortex; pre-SMA, anterior portion of supplementary motor area; Put, putamen; NAcc, nucleus accumbens; STN, subthalamic nucleus; Thal, thalamus; vlPFC, ventrolateral prefrontal cortex; vmPFC, ventromedial prefrontal cortex.
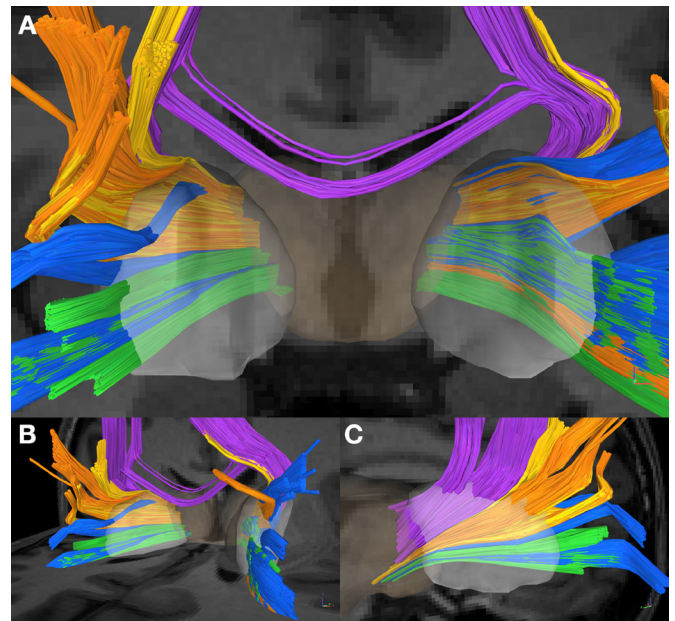


**Figure 3** Thalamocortical streamlines in the anterior limb of the internal capsule (aLIC). Streamlines of a representative subject are rendered with colour-coding for cortical targets (purple: pre-supplementary motor area (pre-SMA), yellow: dorsal cingulate (dACC), orange: dorsolateral prefrontal cortex (dlPFC), blue: ventrolateral prefrontal cortex (vlPFC), green: orbitofrontal cortex (OFC)). Isosurfaces of thalamus (pale brown) and the aLICs (white) are also shown. (A) Front view (radiological orientation), (B) oblique view (from the left), (C) lateral view (from the right).

of the thalamocortical streamlines within the aLICs were consistent with previous studies.[3][4] See figure 3 for thalamocortical streamlines from a representative subject. To quantify the spatial distribution, the centre of gravity in the aLICs in the normalised track-density images was compared between thalamocortical connections (online supplemental table 3). See figure 4 for individual centres of gravity in the aLICs. Subjects with all five thalamocortical connections were used (n=156). Streamlines connecting dorsal and ventral structures were separated. One-way multivariate analysis of variance revealed clear separation in coordinates between cortical targets in the 0-th dimension (ie, group means are not at the same point) and the 1st dimension (ie, group means are not in a straight line) (left, p<0.0001, p<0.0001, p=0.0645; right, p<0.0001, p<0.0001, p=0.3212 for each dimension). Using hierarchical clustering dendrograms based on shortest linkage, bilaterally, the lateral PFC regions are clustered first, followed by clustering with OFC, then dACC and finally pre-SMA (figure 4).

Using model (1), we found significant decreases in FA of streamlines in patients with OCD in all 12 connections tested (p<0.0073, FDR-adjusted) with no differences in NC (p>0.7762, FDR-adjusted) compared with HCs (figure 5).

## Relationship between tractography and capsulotomy outcomes

Using model (2), we found significant correlations between clinical improvement after capsulotomy and NC in the thalamocortical connections of the dlPFC and dACC (r=0.34, p<0.0436). Specifically, Y-BOCS improvements (ie, decreases in Y-BOCS at follow-up compared with baseline) were positively correlated with NC of thalamus–dlPFC (r=0.36, p=0.0347) and thalamus–dACC (r=0.34, p=0.0402) but not with FA (figure 6). We
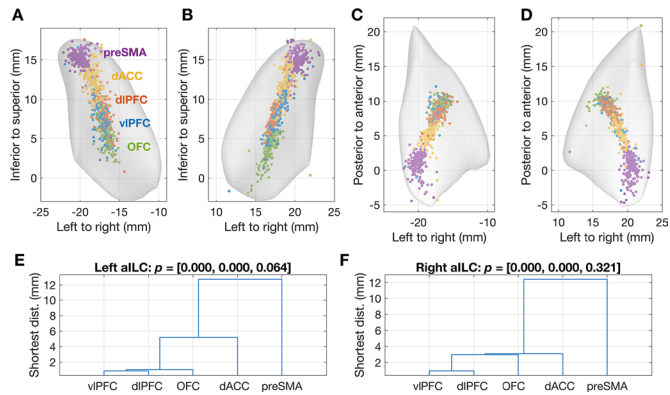
**Figure 4** Centres of gravity and comparison of thalamo–cortical streamlines through the anterior limb of the internal capsule (aLIC) tracts. (A) A rear view of the left aLIC, (B) rear view of the right aLIC, (C) a top view of the left aLIC, (D) a top view of the right aLIC. Each circle represents a centre of gravity of one subject (total n=156) for each thalamocortical connection (purple: pre-SMA, yellow: dACC, orange: dlPFC, blue: vlPFC, green: OFC). Montreal Neurological Institute (MNI) coordinates are marked. (E) A dendrogram of a hierarchical clustering using the single linkage method based on the distances among clusters estimated by a multivariate analysis of variance (MANOVA) model in the left aLIC. (F) A dendrogram for the right aLIC. P values from one-way MANOVA are marked. dACC, dorsal anterior cingulate cortex; dlPFC, dorsolateral prefrontal cortex; OFC, orbitofrontal cortex; pre-SMA, anterior portion of supplementary motor area; vlPFC, ventrolateral prefrontal cortex.

then repeated model (2) with the covariates of time after surgery and changes in scores of depression and anxiety to assess the impact of these factors on our findings. We again show a positive correlation with YBOCS improvement with the NC of thalamus–dlPFC (p=0.016) but the thalamus–dACC results were no longer significant with inclusion of either depression and/or anxiety changes.
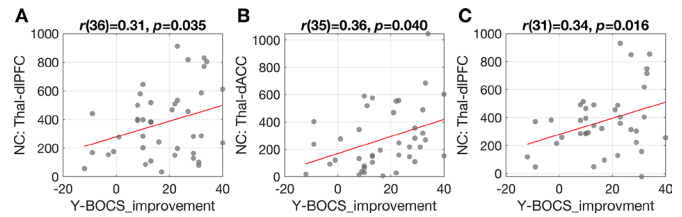


**Figure 6** Correlation between connectivity measures and obsessive-compulsive symptom improvement. (A–B) Correlation between normalised streamline counts (NC) of the dorsolateral prefrontal cortex and thalamus (Thal–dlPFC) and dorsal cingulate and thalamus (Thal–dACC) and improvements of Yale Brown Obsessive Compulsive Symptom (Y-BOCS) scores following capsulotomy (postsurgery and presurgery). (C) Correlation between NC of the thal–dlPFC tracts with the inclusion of clinical variables including improvements in anxiety and depression scores following capsulotomy as covariates. dACC, dorsal anterior cingulate cortex; dlPFC, dorsolateral prefrontal cortex; Thal, thalamus.

## TBSS: whole brain analysis

We further investigated whether these aLIC findings were due to a decrease of FA specifically in the aLIC or whole brain white matter in general, or whether they were specific for thalamo–cortical/striato–cortical streamlines using whole brain TBSS analysis. From the two models (equations 1–2), we only found significant group differences in forceps minor, superior longitudinal fasciculi, and other cerebral and subcortical white matter (p<0.05, threshold free cluster enhancement (TFCE)-corrected). See figure 7 and online supplemental table 4 for significant clusters. We also found decreased FA in a posterior tip of the left aLIC, but very few streamlines pass through this region (0.24%±0.51% of maximal track-density), except thalamus–pre-SMA (25.52%), suggesting that the cluster is at the border as a part of the thalamus–pre-SMA connection and does not overlap with other streamlines. There was no correlation between TBSS and clinical outcome measures. Therefore, the TBSS analysis confirmed that the tractography was not confounded by the common seed (ie, aLIC) but specifically quantified structural connectivity of the thalamo–cortical/striato–cortical tracts.
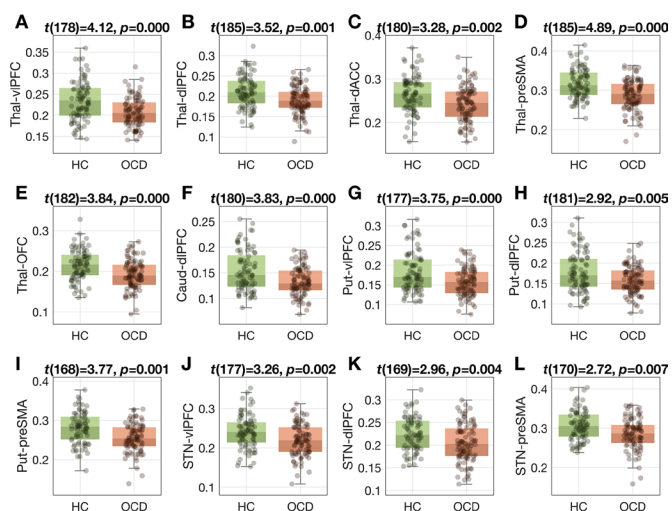


**Figure 5** Group differences in fractional anisotropy in all connections tested (A–L). HC, healthy control, OCD, obsessive-compulsive disorder. P values are adjusted by false discovery rate (FDR). dACC, dorsal anterior cingulate cortex; dlPFC, dorsolateral prefrontal cortex; OFC, orbitofrontal cortex; pre-SMA, anterior portion of supplementary motor area; STN, subthalamic nucleus; vlPFC, ventrolateral prefrontal cortex.
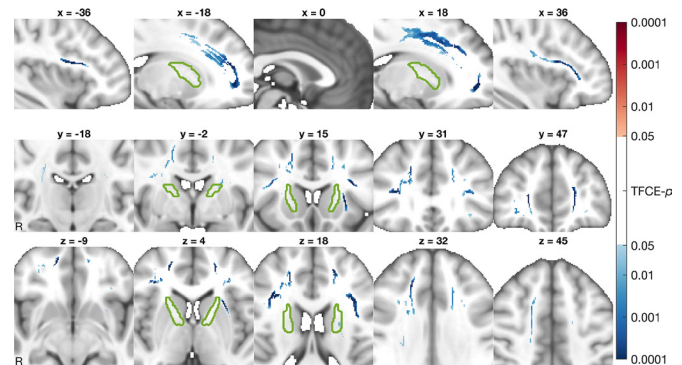


**Figure 7** Voxel-wise group differences in fractional anisotropy (FA). Using tract-based spatial statistics, FA values were compared and thresholded at p<0.05 (TFCE corrected). Signed p values are visualised in a log-scale for a contrast of patients with obsessive-compulsive disorder (OCD) minus healthy controls (HCs). Reddish colours mark increases while bluish colours mark decreases in OCDs compared with HCs. Green contours mark anterior limbs of internal capsules.

## DISCUSSION

In this large-scale diffusion-weighted study, we focus on prefrontal–subcortical streamlines coursing through the aLIC highlighting differences between OCD subjects and healthy controls and showing a potential relationship with capsulotomy outcomes. We first show that compared with healthy controls, OCD was associated with lower FA in the aLIC across multiple prefrontal cortico-thalamic and cortico–striatal streamlines, namely bilateral dlPFC, vlPFC, dorsal cingulate, pre-SMA, OFC and vmPFC. Similarly, lower prefrontal–subthalamic streamlines from dlPFC, vlPFC and pre-SMA were observed possibly reflecting hyper-direct projections. Critically, these findings may be specific to these prefrontal–subcortical streamlines coursing through the aLIC as whole-brain TBSS showed the aLIC in OCD to be no different from healthy controls, except in a posterior region with limited prefrontal–subcortical tracts. Instead, the TBSS analysis highlighted lower FA in various prefrontal regions including the connection between frontopolar hemispheres (forceps minor), streamlines within insular and middle frontal gyrus, and the long-range superior longitudinal fasciculus linking posterior and anterior cerebral regions of parieto-occipital and fronto-temporal cortices.

Critically, we highlight a relationship between presurgical aLIC-tractography and capsulotomy outcomes with higher streamline count in the dlPFC–thalamic tracts predicting greater obsessive-compulsive symptom improvement post-capsulotomy. We show a potential dissociation between improvements in obsessive-compulsive symptoms as compared with anxious-depression symptoms with greater streamline count in the dACC–thalamic tracts predicting surgical outcome but likely mediated by greater improvements in anxiety or depressive symptomatology, features commonly comorbid in OCD.

### Anatomical organisation of prefrontal–thalamic tracts in the aLIC

Across all subjects, we show an anterior–posterior ventral–dorsal axis organisation demonstrating clustering of lateral prefrontal tracts and dissociating from ventral and dorsal prefrontal tracts. These findings have relevance to potential neurosurgical targeting influencing differing prefrontal regions. A DTI study in primates and human subjects that segmented human aLIC into five regions based on the positions of axons from different cortical regions[4] revealed that fibres from vmPFC, dorsomedial PFC, dACC, vlPFC and dlPFC have some degree of topographical arrangement within the aLIC. This finding is homologous with rodent studies demonstrating that descending PFC fibres in the form of white-matter fascicles embedded within the striatum are arranged topographically.[34]

Here, we confirm a statistically significant topographical arrangement based on functionally defined prefrontal regions and further show that within the aLIC a hierarchical clustering anatomical organisation: the lateral prefrontal cortices appear to cluster together, followed by OFC, then dACC and finally pre-SMA. This clustering arrangement has implications for DBS targeting and contact stimulation or more precise ablative lesioning within the aLIC. For instance, our findings suggest that a ventral anterior target (volume of tissue activation or lesion) of the aLIC is likely to simultaneously influence both dorsolateral and ventrolateral prefrontal cortices and may be difficult to dissociate in the context of precision targeting. Greater extension in the aLIC may then involve OFC with a more ventrally and anteriorly extension or contact then influencing dACC and pre-SMA.

### Dorsolateral prefrontal cortex: capsulotomy outcomes

Our findings highlight a relationship between dlPFC and capsulotomy outcome: OCD subjects with higher dlPFC–thalamic streamline counts have better obsessive-compulsive symptom improvement outcomes after capsulotomy controlled for anxiety and depression scores. This finding highlighting the dlPFC tracts is consistent with observations from DBS studies. Obsessive-compulsive symptomatology improvement after VIC DBS in OCD was predicted by DBS contacts specifically targeting dlPFC tracts.[17 18] The effect of VIC DBS has also been suggested to be partly explained by the enhancement of cognitive control involving prefrontal regions including the dlPFC.[35] Furthermore, in a DBS study targeting the anterior limbic-associative STN in OCD, stimulation was associated with an improvement in reflection impulsivity correlating with dlPFC and STN resting state functional connectivity.[21]

Here we show that FA of the dlPFC is lower in patients with OCD relative to healthy controls, but no differences were observed in streamline counts. These FA findings are consistent with observations of impairments of the dlPFC in OCD particularly with impaired functioning in goal-directed control,[36–39] working memory,[40] strategic planning[36] and reflection impulsivity.[39] However, the count of dlPFC–thalamic streamlines was not a marker for the differences between OCD relative to healthy controls nor a marker of baseline severity. As the location of capsulotomy is highly likely to target these dlPFC-tracts, those with a greater baseline number of streamlines may have a greater sensitivity and capacity for postsurgical plasticity or reorganisation and hence symptom improvement. The final common mechanisms underlying stimulation and reorganisation post-capsulotomy might overlap, suggesting that the thalamic-dlPFC tracts may be important for optimal clinical outcome. Further longitudinal studies are required to address these specific questions.

### Dorsal cingulate: capsulotomy outcomes

We further show that greater counts of thalamic–dorsal cingulate streamlines are also related with capsulotomy outcomes but suggest this may be mediated by improvements in anxiety and depressive symptoms. The dorsal cingulate is commonly implicated in OCD pathophysiology involving enhanced error monitoring with a greater error related negativity[41] and greater aversive processing.[42]

The dorsal cingulate, and more specifically the rostral cingulate and mesial prefrontal cortex at the genu of the corpus callosum was implicated in a tractography study predicting the clinical improvement of obsessive-compulsive symptoms for both DBS targeting the VIC and the STN.[18] Cingulotomy targeting the cingulum bundle has also shown efficacy in alleviating treatment refractory OCD.[14] We have previously shown that resting state functional connectivity of the dorsal cingulate and striatum was decreased in patients with OCD following capsulotomy and that connectivity predicted improvement of obsessive-compulsive scores 1 month post-capsulotomy.[19] We have also shown normalisation and improvement of postoperative glucose metabolism in dorsal cingulate, OFC, caudate and thalamus following OCD capsulotomy in eight patients, regions which were hypometabolic presurgery relative to healthy controls.[43] Our current finding differs from these previous predictive studies[18 19] in highlighting the role of depressive and anxiety symptoms which may be related to our inclusion of anxiety assessments, differences between neurosurgical procedures (DBS and capsulotomy) or methodological and clinical outcomes (resting state fMRI 1 month after

surgery as compared with tractography 6 months after surgery). These findings focusing on depressive improvements are consistent with a dual stimulation study in OCD demonstrating that tracts from the VIC DBS target were associated with the medial OFC and vmPFC linked with improving depressive symptoms whereas STN DBS tracts were associated with other prefrontal regions linked with improving behavioural flexibility.[44] Further studies focusing on linking cognitive processes and anatomical targets on postsurgical outcomes are indicated.

## Limitations and summary

This study is not without limitations. First, we note that specific conventional DTI processing steps such as Eddy current correction are not appropriate for DSI data. Second, as the frontal SNR was low, a high-order model such as generalised q-sampling imaging[25] resulted in implausible results. Therefore, we limited ourselves to a traditional Gaussian tensor model, which is more robust to noise. Third, even though, poor SNR may still have limited the identification of these tracts to thalamic or subthalamic nuclei; in some cases of subcortical–cortical pairs, no streamline was found in some subjects. Thus, we only performed group-wise analyses for those ROI pairs, for which streamlines revealed in more than 90% of subjects. Alternative ROIs using Brodmann Areas were considered but did not result in more streamlines that allows comparisons between all possible subcortico–cortical pairs. This limitation excluded many of interesting subcortical regions such as NAcc and medial/lateral OFC[44] from the current analyses. In exploration, we conducted a separate analysis of the vmPFC and NAcc (see online supplemental materials and figure 4) without constraining within the aLIC ROI. The streamlines were found in 89% of subjects and consistent with the anatomy of vmPFC tracts[45 46] but did not necessarily pass through the aLIC ROI. Data with higher SNR are necessary to enable more comprehensive analysis. Fourth, the current study was based on the assumption that the aLIC regions are similarly affected in patients who underwent capsulotomy. This assumption should be confirmed by post-capsulotomy images, which are still in the process. However, in a separate study, we reported the relationship between OCD improvement and the lesion size and location using structural images acquired 1–5 months after surgery[47] (see online supplemental figure 5 for the overlap between the aLIC seed masks in the current study and the lesion probability map from a subset of patients from the separate study[47]). A coming study will be able to stratify patients based on actual lesion sites (thus affected white matter tracts).

In conclusion, the current findings shed light on the pathophysiology of OCD and therapeutic mechanisms of capsulotomy and may contribute towards precision targeting as a function of dimensional symptoms to optimise outcomes in OCD.[20 48] Understanding the differential functional role of cortico–subcortical tracts further highlights the symptom dimensional relevance of treatment targets for both invasive and non-invasive neuromodulation across other psychiatric disorders.

## Author affiliations

[1]Department of Neurosurgery, Center for Functional Neurosurgery, Shanghai Jiao Tong University Medical School Affiliated Ruijin Hospital, Shanghai, China
[2]Department of Psychiatry, Cambridge University, Cambridge, UK
[3]Department of Psychology and Neuroscience, Duke University, Durham, North Carolina, USA
[4]Institute of Neuroscience, State Key Laboratory of Neuroscience, Shanghai, China
[5]University of the Chinese Academy of Sciences, Beijing, China
[6]Department of Psychiatry, Pudong District Mental Health Center, Shanghai, China
[7]Institute for Medical Imaging Technology, School of Biomedical Engineering, Shanghai Jiao Tong University, Shanghai, China
[8]Department of Psychiatry, Zhongshan Hospital Fudan University, Shanghai, China
[9]Institute of Neuroscience, State Key Laboratory of Neuroscience, CAS Center for Excellence in Brain Science and Intelligence Technology, CAS Key Laboratory of Primate Neurobiology, Chinese Academy of Sciences, Shanghai, China

**ORCID iDs**
Chencheng Zhang http://orcid.org/0000-0003-4472-4134
Jun Li http://orcid.org/0000-0002-4589-7371

## REFERENCES

1. Burguière E, Monteiro P, Mallet L, *et al*. Striatal circuits, habits, and implications for obsessive-compulsive disorder. *Curr Opin Neurobiol* 2015;30:59–65.
2. Robbins TW, Vaghi MM, Banca P. Obsessive-Compulsive disorder: puzzles and prospects. *Neuron* 2019;102:27–47.
3. Nanda P, Banks GP, Pathak YJ, *et al*. Connectivity-based parcellation of the anterior limb of the internal capsule. *Hum Brain Mapp* 2017;38:6107–17.
4. Safadi Z, Grisot G, Jbabdi S, *et al*. Functional segmentation of the anterior limb of the internal capsule: linking white matter abnormalities to specific connections. *J Neurosci* 2018;38:2106–17.
5. Koch K, Reess TJ, Rus OG, *et al*. Diffusion tensor imaging (DTI) studies in patients with obsessive-compulsive disorder (OCD): a review. *J Psychiatr Res* 2014;54:26–35.
6. Gan J, Zhong M, Fan J, *et al*. Abnormal white matter structural connectivity in adults with obsessive-compulsive disorder. *Transl Psychiatry* 2017;7:e1062.
7. Szeszko PR, Ardekani BA, Ashtari M, *et al*. White matter abnormalities in obsessive-compulsive disorder: a diffusion tensor imaging study. *Arch Gen Psychiatry* 2005;62:782–90.
8. Lochner C, Fouché J-P, du Plessis S, *et al*. Evidence for fractional anisotropy and mean diffusivity white matter abnormalities in the internal capsule and cingulum in patients with obsessive-compulsive disorder. *J Psychiatry Neurosci* 2012;37:193–9.
9. Cannistraro PA, Makris N, Howard JD, *et al*. A diffusion tensor imaging study of white matter in obsessive-compulsive disorder. *Depress Anxiety* 2007;24:440–6.

10  Mallet L, Polosan M, Jaafari N, *et al*. Subthalamic nucleus stimulation in severe obsessive-compulsive disorder. *N Engl J Med* 2008;359:2121–34.

11  Greenberg BD, Gabriels LA, Malone DA, *et al*. Deep brain stimulation of the ventral internal capsule/ventral striatum for obsessive-compulsive disorder: worldwide experience. *Mol Psychiatry* 2010;15:64–79.

12  Miguel EC, Lopes AC, McLaughlin NCR, *et al*. Evolution of gamma knife capsulotomy for intractable obsessive-compulsive disorder. *Mol Psychiatry* 2019;24:218–40.

13  Denys D, Mantione M, Figee M, *et al*. Deep brain stimulation of the nucleus accumbens for treatment-refractory obsessive-compulsive disorder. *Arch Gen Psychiatry* 2010;67:1061–8.

14  Brown LT, Mikell CB, Youngerman BE, *et al*. Dorsal anterior cingulotomy and anterior capsulotomy for severe, refractory obsessive-compulsive disorder: a systematic review of observational studies. *J Neurosurg* 2016;124:77–89.

15  Kumar KK, Appelboom G, Lamsam L, *et al*. Comparative effectiveness of neuroablation and deep brain stimulation for treatment-resistant obsessive-compulsive disorder: a meta-analytic study. *J Neurol Neurosurg Psychiatry* 2019;90:469–73.

16  Rasmussen SA, Noren G, Greenberg BD, *et al*. Gamma ventral capsulotomy in intractable obsessive-compulsive disorder. *Biol Psychiatry* 2018;84:355–64.

17  Baldermann JC, Melzer C, Zapf A, *et al*. Connectivity profile predictive of effective deep brain stimulation in obsessive-compulsive disorder. *Biol Psychiatry* 2019;85:735–43.

18  Li N, Baldermann JC, Kibleur A. Toward a unified connectomic target for deep brain stimulation in obsessive-compulsive disorder. *bioRxiv*2019;608786.

19  Yin D, Zhang C, Lv Q, *et al*. Dissociable Frontostriatal connectivity: mechanism and predictor of the clinical efficacy of capsulotomy in obsessive-compulsive disorder. *Biol Psychiatry* 2018;84:926–36.

20  Voon V. Toward precision medicine: prediction of deep brain stimulation targets of the ventral internal capsule for obsessive-compulsive disorder. *Biol Psychiatry* 2019;85:708–10.

21  Voon V, Droux F, Morris L, *et al*. Decisional impulsivity and the associative-limbic subthalamic nucleus in obsessive-compulsive disorder: stimulation and connectivity. *Brain* 2017;140:442–56.

22  Morris LS, Kundu P, Dowell N, *et al*. Fronto-striatal organization: defining functional and microstructural substrates of behavioural flexibility. *Cortex* 2016;74:118–33.

23  Tuch DS, Reese TG, Wiegell MR, *et al*. Diffusion MRI of complex neural architecture. *Neuron* 2003;40:885–95.

24  Manjón JV, Coupé P, Concha L, *et al*. Diffusion weighted image denoising using overcomplete local PCA. *PLoS One* 2013;8:e73021.

25  Yeh F-C, Wedeen VJ, Tseng W-YI. Generalized q-sampling imaging. *IEEE Trans Med Imaging* 2010;29:1626–35.

26  Yeh F-C, Verstynen TD, Wang Y, *et al*. Deterministic diffusion fiber tracking improved by quantitative anisotropy. *PLoS One* 2013;8:e80713.

27  Descoteaux M, Deriche R, Knösche TR, *et al*. Deterministic and probabilistic tractography based on complex fibre orientation distributions. *IEEE Trans Med Imaging* 2009;28:269–86.

28  Desikan RS, Ségonne F, Fischl B, *et al*. An automated labeling system for subdividing the human cerebral cortex on MRI scans into gyral based regions of interest. *Neuroimage* 2006;31:968–80.

29  Xiao Y, Beriault S, Pike GB, *et al*. Multicontrast multiecho FLASH MRI for targeting the subthalamic nucleus. *Magn Reson Imaging* 2012;30:627–40.

30  Malone IB, Leung KK, Clegg S, *et al*. Accurate automatic estimation of total intracranial volume: a nuisance variable with less Nuisance. *Neuroimage* 2015;104:366–72.

31  Belsley DA, Kuh E, Welsch RE. *Regression diagnostics: identifying influential data and sources of collinearity*. John Wiley & Sons, 2005.

32  Smith SM, Jenkinson M, Johansen-Berg H, *et al*. Tract-based spatial statistics: voxelwise analysis of multi-subject diffusion data. *Neuroimage* 2006;31:1487–505.

33  Smith SM, Nichols TE. Threshold-free cluster enhancement: addressing problems of smoothing, threshold dependence and localisation in cluster inference. *Neuroimage* 2009;44:83–98.

34  Coizet V, Heilbronner SR, Carcenac C, *et al*. Organization of the anterior limb of the internal capsule in the rat. *J Neurosci* 2017;37:2539–54.

35  Widge AS, Zorowitz S, Basu I, *et al*. Deep brain stimulation of the internal capsule enhances human cognitive control and prefrontal cortex function. *Nat Commun* 2019;10:1536.

36  Vaghi MM, Vértes PE, Kitzbichler MG, *et al*. Specific Frontostriatal circuits for impaired cognitive flexibility and goal-directed planning in obsessive-compulsive disorder: evidence from resting-state functional connectivity. *Biol Psychiatry* 2017;81:708–17.

37  Voon V, Derbyshire K, Rück C, *et al*. Disorders of compulsivity: a common bias towards learning habits. *Mol Psychiatry* 2015;20:345–52.

38  Gillan CM, Papmeyer M, Morein-Zamir S, *et al*. Disruption in the balance between goal-directed behavior and habit learning in obsessive-compulsive disorder. *Am J Psychiatry* 2011;168:718–26.

39  Voon V, Reiter A, Sebold M, *et al*. Model-Based control in dimensional psychiatry. *Biol Psychiatry* 2017;82:391–400.

40  Nakao T, Nakagawa A, Nakatani E, *et al*. Working memory dysfunction in obsessive-compulsive disorder: a neuropsychological and functional MRI study. *J Psychiatr Res* 2009;43:784–91.

41  Riesel A, Endrass T, Kaufmann C, *et al*. Overactive error-related brain activity as a candidate endophenotype for obsessive-compulsive disorder: evidence from unaffected first-degree relatives. *Am J Psychiatry* 2011;168:317–24.

42  Apergis-Schoute AM, Gillan CM, Fineberg NA, *et al*. Neural basis of impaired safety signaling in obsessive compulsive disorder. *Proc Natl Acad Sci U S A* 2017;114:3216–21.

43  Zuo C, Ma Y, Sun B, *et al*. Metabolic imaging of bilateral anterior capsulotomy in refractory obsessive compulsive disorder: an FDG PET study. *J Cereb Blood Flow Metab* 2013;33:880–7.

44  Tyagi H, Apergis-Schoute AM, Akram H, *et al*. A randomized trial directly comparing ventral capsule and anteromedial subthalamic nucleus stimulation in obsessive-compulsive disorder: clinical and imaging evidence for dissociable effects. *Biol Psychiatry* 2019;85:726–34.

45  Lehman JF, Greenberg BD, McIntyre CC, *et al*. Rules ventral prefrontal cortical axons use to reach their targets: implications for diffusion tensor imaging tractography and deep brain stimulation for psychiatric illness. *J Neurosci* 2011;31:10392–402.

46  Jbabdi S, Lehman JF, Haber SN, *et al*. Human and monkey ventral prefrontal fibers use the same organizational principles to reach their targets: tracing versus tractography. *J Neurosci* 2013;33:3190–201.

47  Lv Q, Lv Q, Yin D, *et al*. Neuroanatomical substrates and predictors of response to capsulotomy in intractable obsessive-compulsive disorder. *Biol Psychiatry Cogn Neurosci Neuroimaging* 2020. doi:10.1016/j.bpsc.2020.05.005. [Epub ahead of print: 20 May 2020].

48  Dougherty DD. Will deep brain stimulation help move precision medicine to the clinic in psychiatry? *Biol Psychiatry* 2019;85:706–7.